Synthesis and Crosslinking of Hyperbranched Poly(*n*-nonyl acrylate) to Form Organogels

Yangtian Lu,[1] Dibyendu Debnath,[1] R. A. Weiss,[2] Coleen Pugh[1]

[1]Department of Polymer Science, University of Akron, Akron, Ohio 44325-3909
[2]Department of Polymer Engineering, University of Akron, Akron, Ohio 44325-3909
Correspondence to: R. A. Weiss (E-mail: rweiss@uakron.edu) or C. Pugh (E-mail: cpugh@uakron.edu)

Received 30 October 2014; accepted 25 April 2015; published online 3 June 2015
DOI: 10.1002/pola.27700

ABSTRACT: (2-Bromo-*n*-nonan-1-oxycarbonyl)ethyl acrylate was synthesized as an inimer for self-condensing vinyl polymerization (SCVP) to produce hyperbranched poly(*n*-nonyl acrylate), either as a homopolymer or as a copolymer with *n*-nonyl acrylate. The inimer was homopolymerized and copolymerized by atom transfer radical polymerization (ATRP) and activator generated by electron transfer ATRP to produce soluble polymers with broad polydispersities (up to $Đ = 9.91$), which is characteristic of hyperbranched polymers produced by SCVP. The resulting hyperbranched (co)polymers were crosslinked by atom transfer radical coupling in both one-pot and two-step procedures. The radical–radical crosslinking reaction is extremely efficient, resulting in hard plastic particles from the homopolymer of (2-bromo-*n*-nonan-1-oxycarbonyl)ethyl acrylate synthesized in bulk. Crosslinked organogels that swell in tetrahydrofuran were formed when the rate of crosslinking decreased using acetonitrile solutions. Dynamic shear and stress relaxation experiments demonstrated that the dry network behaves as a covalently crosslinked soft gel, with a glass transition at −50 °C according to differential scanning calorimetry. © 2015 Wiley Periodicals, Inc. J. Polym. Sci., Part A: Polym. Chem. **2015**, *53*, 2399–2410

KEYWORDS: gels; hydrophobic; hyperbranched polymer; inimer; organogel; polyacrylates

INTRODUCTION Atom transfer radical polymerization (ATRP)[1,2] is a versatile method for the polymerization of a wide range of monomers, including (meth)acrylates,[3] to produce novel well-defined polymers. ATRP can also be applied to self-condensing vinyl polymerizations (SCVPs),[4] which provide a convenient, one-batch synthesis of hyperbranched polymers.[5–7] Recently, we designed a new type of acrylate inimer[8,9] that produces hyperbranched polyacrylates by ATRP.[10] These acrylate inimers were designed to produce nearly exact architectural analogs of the corresponding linear polyacrylate, with an ester group attached to every other carbon atom along the polymer backbone and a nonfunctionalized alkyl ester attached as a free pendant group. Because of the chemical similarity of these branched polyacrylates and their linear analogs, their ^{1}H and ^{13}C NMR spectra are nearly identical, with no unique resonances for the branch points. Nevertheless, the hyperbranched architecture is supported by the characteristically broad molecular weight distributions throughout the polymerization;[10] by the significant underestimation in their molecular weights measured by gel permeation chromatography relative to a linear standard;[10] and by two-dimensional mass spectrometry characterization;[11] however, none of these techniques are quantitative.

The ATRP of these acrylate inimers is slow, especially with bulky ester substituents. Recently, Jakubowski and Matyjaszewski proposed an activator generated by electron transfer (AGET) ATRP system that uses a standard ATRP initiator and a higher oxidation state transition metal complex ($X–Mt^{n+1}/L$);[12] the higher oxidation state transition metal complex is converted to the activator (Mt^{n}) by reaction with a reducing agent such as ascorbic acid. This method has the characteristics of normal ATRP, but with the added benefit that it uses a more oxidatively stable catalyst complex in the reaction mixture. The current article describes the use of an AGET ATRP system, in addition to traditional ATRP, for the SCVP of an acrylate inimer with a bulky *n*-nonyl ester substituent (Scheme 1).

The simulations of the kinetics of SCVP proposed by Müller and coworkers demonstrated that SCVP produces polymers with a high degree of branching and numerous initiating sites at high conversion.[13,14] Therefore, SCVPs of the acrylate inimers produce hyperbranched polyacrylates with many halogen atoms throughout each molecule. We previously limited the acrylate inimer conversions to 80–90% to prevent crosslinking by inevitable radical–radical coupling.[10] The high concentration of halogen atoms throughout the hyperbranched structure should provide an ideal route for crosslinking these polymers by radical–radical coupling reactions

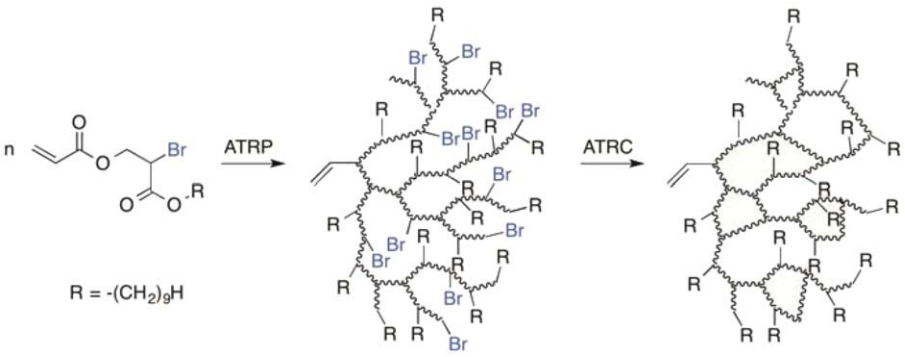

SCHEME 1 Synthesis and crosslinking of hyperbranched poly(*n*-nonyl acrylate); only intramolecular crosslinking is shown. [Color figure can be viewed in the online issue, which is available at wileyonlinelibrary.com.]

to prepare crosslinked systems such as gels. Polymeric gels are solvent-swollen systems in which the polymer is physically or chemically crosslinked to form a three-dimensional network. Gels have attracted considerable attention because of their many applications, including the encapsulation and delivery of drugs.[15,16] Covalent crosslinking affects many important physical properties such as the modulus, thermal response, solvent/water ingress, and fracture behavior.[17] These crosslinked networks do not dissolve in any solvent, but rather swell on solvent adsorption.

The hyperbranched polyacrylates reported in this study with hydrophobic *n*-nonyl substituents should be useful for preparing organogels. Organogels[18,19] are a special class of gels that swell in the presence of an organic solvent. Although the chemical composition of the gel determines which solvents will cause swelling, the molecular architecture of the gel determines its absorption capacity. For example, Wu et al.[20] reported that complexes of sulfonated poly[styrene-*block*-(ethylene-*ran*-butylene)-*block*-styrene] and a polypropylenimine dendrimer can absorb 22 times its weight in diesel and in toluene. Organogels are useful for a variety of applications, including dermal drug delivery, such as with a lecithin-based organogel;[21] colorimetric detection of ions, such as fluoride ions using a poly(aryl ether) dendritic organogel connected to an anthracene chromophore through acylhydrazone linkages;[22] and fluorometric detection of small molecules, such as aliphatic amines using a naphthalimide-containing organogel.[23] Thermoresponsive organogels can also be formed by complexing a polyelectrolyte with an oppositely charged surfactant.[24]

As the hyperbranched polyacrylates contain abundant halogen atoms throughout their structure, they may produce organogels by atom transfer radical coupling[25] (ATRC) using an efficient reducing agent (Scheme 2). Linear polystyrene and poly(methyl acrylate) (PMA) with halogenated end groups can be coupled by radical–radical coupling in high efficiency (99%);[26,27] even poly(methyl methacrylate) radicals can be coupled if styrene is first added to the terminal halide unit.[28] Although the equilibrium constant for radical formation is 100 times lower[29] for PMA-Br than polystyrene-Br, and the rate of linear PMA radical–radical coupling is therefore very slow,[19] this study will demonstrate that the rate of radical–radical coupling in hyperbranched poly(*n*-nonyl acrylate)s is highly efficient and useful for crosslinking. Although the radical–radical coupling reaction can be influenced by altering the solvent polarity, our objective is to synthesize a hyperbranched polyacrylate-based organogel with high absorption for organic solvents.

EXPERIMENTAL

Materials

Acrylic acid (99%; Aldrich), acryloyl chloride (99%; Aldrich), anisole (99.7%; Aldrich), L-ascorbic acid (Fisher), cupric bromide (99%; Aldrich), HBr (~48 wt %; Acros), $NaNO_2$ (97%; Fisher), $NaHCO_3$ (99.7%; Mallinakrodt), NaBr (98%; Acros), methanol (99.8%; Aldrich), *n*-nonanol (98%; Sigma), *N*,*N*,*N*′,*N*″,*N*″-pentamethyldiethylenetriamine (PMDETA, 99%; Aldrich), D,L-serine (98%; Aldrich), and *p*-toluenesulfonic acid (Fisher) were used as received. Acrylic anhydride (19–55% yield), 2-bromo-3-hydroxypropionic acid (40% yield), and (2-bromo-2-methoxycarbonyl)ethyl acrylate (55–61% yield) were synthesized as described previously.[9] Azobisisobutyronitrile (AIBN, 99.7%; Sigma Aldrich) was recrystallized from methanol below 40 °C. Cuprous bromide (98%; Aldrich) was purified by stirring it in glacial acetic acid overnight, washing it several times with methanol, and then drying.[30] Diethyl ether was dried by distillation from purple sodium benzophenone ketyl under N_2. Benzene was distilled from CaH_2. Reagent-grade tetrahydrofuran (THF) was dried by distillation from purple sodium benzophenone ketyl under N_2. Triethylamine (99%; Aldrich) was distilled from KOH under nitrogen.

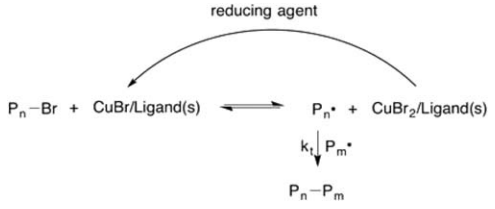

SCHEME 2 Mechanism for atom transfer radical coupling (ATRC).

Techniques

All reactions were performed under a N_2 atmosphere using a Schlenk line unless noted otherwise. In some cases, polymerizations were performed in what will be referred to as a "vial reactor," created by covering a 20-mL glass-threaded vial with an upside–down rubber septum, piercing the septum with a short needle, and then covering the pierced septum with a 14/20 gas adapter, which can then be attached to the Schlenk line. Thin-layer chromatography was performed using silica gel plates (200 μm particle size w/ UV254; Sorbent Technologies) with a polyester backing.

^{1}H (300 MHz) and ^{13}C (75 MHz) NMR spectra (δ, ppm) were recorded on a Varian Mercury 300 instrument. All spectra were recorded in $CDCl_3$, and the resonances were measured relative to residual solvent resonances and referenced to tetramethylsilane (0.00 ppm). Number–average (M_n) and weight–average (M_w) molecular weights relative to linear polystyrene [gel permeation chromatography (GPC_{PSt})] and polydispersities ($Đ = M_w/M_n$) were determined by GPC from calibration curves of log M_n versus elution volume at 35 °C using THF as solvent (1.0 mL/min), a guard column and set of 50 Å, 100 Å, 10^4 Å, and linear (50–10^4 Å) Styragel 5 μm columns, a Waters 486 tunable UV/vis detector set at 254 nm, a Waters 410 differential refractometer, and Millenium Empower 2 software. The samples (~0.1 g/L) were dissolved overnight and filtered through a 0.45-μm PTFE filter.

A TA Q200 differential scanning calorimeter was used to determine the glass transition temperature of a 3.99 mg sample of dry gel, which was read as the middle of the change in heat capacity. All heating and cooling rates were 10 °C/min. The transition temperature was calibrated using an indium standard. Thermogravimetric analysis (TGA) of a 3.01 mg dry gel sample was performed with a TA Q50 instrument from room temperature to 700 °C at a heating rate of 10 °C/min under a continuous flow (50 mL/min) of air. Wide-angle X-ray diffraction was performed on a Rigaku Rapid II diffractometer with an image-plate area detector and a tube-anode X-ray generator (Cu Kα radiation) operated at 40 kV and 30 mA ($\lambda = 1.5418$ Å). Powder diffraction patterns were collected in reflection geometry on a fixed χ-axis (45°) goniometer continuously spinning around the φ-axis. The intensity–2θ plots were obtained via azimuthal integration of the two-dimensional diffraction pattern with a 2θ resolution of 0.10. Peak positions were calibrated using silicon powder as the standard.

Dynamic shear and stress relaxation experiments were conducted with an ARES G2 rheometer (TA Instruments) using an 8-mm-diameter parallel-plate geometry. Frequency sweeps with 1% strain were used to measure the linear dynamic shear properties of the dry polymer. Strain sweeps at a frequency of 0.25 rad/s indicated that the linear region extended to ~20% strain. Disk-shaped samples of approximately 8-mm-diameter were die-cut and placed between the plates with a gap of 2.14 mm. The sample was equilibrated for 30 min until the normal force achieved a constant value of 0.205 N, after which the viscoelastic properties were measured at 25 °C, covering an angular frequency (ω) range of 10^{-3} to 10^2 rad/s. Stress relaxation experiments were measured on similar samples as those used for the dynamic shear experiments. A constant strain of 10% was used, and the time-dependent torque, from which the time-dependent shear stress was calculated, was measured from 0.02 s to as long as 13.3 h at constant temperatures of 25, 50, 75, and 100 °C.

Synthesis of n-Nonyl 2-Bromo-3-hydroxypropionate by Esterification of 2-Bromo-3-hydroxypropionic Acid with n-Nonanol

A solution of 2-bromo-3-hydroxypropionic acid (18 g, 0.11 mol), *n*-nonanol (19 g, 0.13 mol), and *p*-toluenesulfonic acid (81 mg, 0.47 mmol) in dry benzene (50 mL) was stirred at 75–80 °C for 45 h while collecting the benzene–water azeotrope in a Dean-Stark trap. After cooling to room temperature, CH_2Cl_2 (200 mL) was added, and the organic phase was washed three times with 4 wt % aqueous $NaHCO_3$ (50 mL each) and once with saturated aqueous NaCl (50 mL), and then dried over Na_2SO_4. After filtration and removing the solvent by rotary evaporation, 32 g (69%) of crude product was obtained as a slightly yellow liquid, and the product was purified by column chromatography ($R_f = 0.15$) using silica gel as the stationary phase and CH_2Cl_2/Et_2O (95:5 v/v) as the eluant to obtain 22 g (48% yield) of *n*-nonyl 2-bromo-3-hydroxypropionate as a colorless oil. The ^{1}H NMR spectrum in Figure 1 demonstrates that *n*-nonyl 2-bromo-3-hydroxypropionate is contaminated with a small amount of an ester (small resonances *a*′, *b*′, and *c*′) formed by a second esterification with 2-bromo-3-hydroxypropionic acid. This oligomer could not be separated from *n*-nonyl 2-bromo-3-hydroxypropionate by column chromatography using a range of eluants: hexanes ($R_f = 0$), 9:1 (v:v) hexanes/THF ($R_f = 0$), CH_2Cl_2 ($R_f = 0.08$), $CHCl_3$ ($R_f = 0.10$), 9:1 (v:v) $CHCl_3/Et_2O$ ($R_f = 0.18$), 9:1 (v:v) CH_2Cl_2/Et_2O ($R_f = 0.35$), 1:1 (v:v) hexanes/ethyl acetate ($R_f = 0.40$), 1:1 (v:v) hexanes/THF ($R_f = 0.43$), 1:1 (v:v) CH_2Cl_2/Et_2O ($R_f = 0.50$), 9:1 (v:v) CH_2Cl_2/THF ($R_f = 0.5$–0.8), THF ($R_f = 0.60$), and Et_2O ($R_f = 0.68$). *n*-Nonyl 2-bromo-3-hydroxypropionate was therefore used in the next step without further purification, and the oligomer was removed when the inimer was purified.

Synthesis of (2-Bromo-2-n-nonan-1-oxycarbonyl)ethyl Acrylate

Two solutions of acrylic anhydride (9.3 g, 74 mmol) in THF (50 mL) and of triethylamine (7.4 g, 73 mmol) in THF (50 mL) were simultaneously added dropwise over 4 min to an ice-cooled solution of nonyl 2-bromo-3-hydroxypropionate (21 g, 72 mmol) in THF (50 mL). After stirring the reaction mixture at room temperature for 15 h, it was poured into ice water (150 mL), and the resulting mixture was stirred for 1 h. THF was removed by rotary evaporation. As the product formed an oil rather than precipitating as a solid from the remaining aqueous mixture, the organic mixture was extracted four times (50 mL each) with CH_2Cl_2. The combined

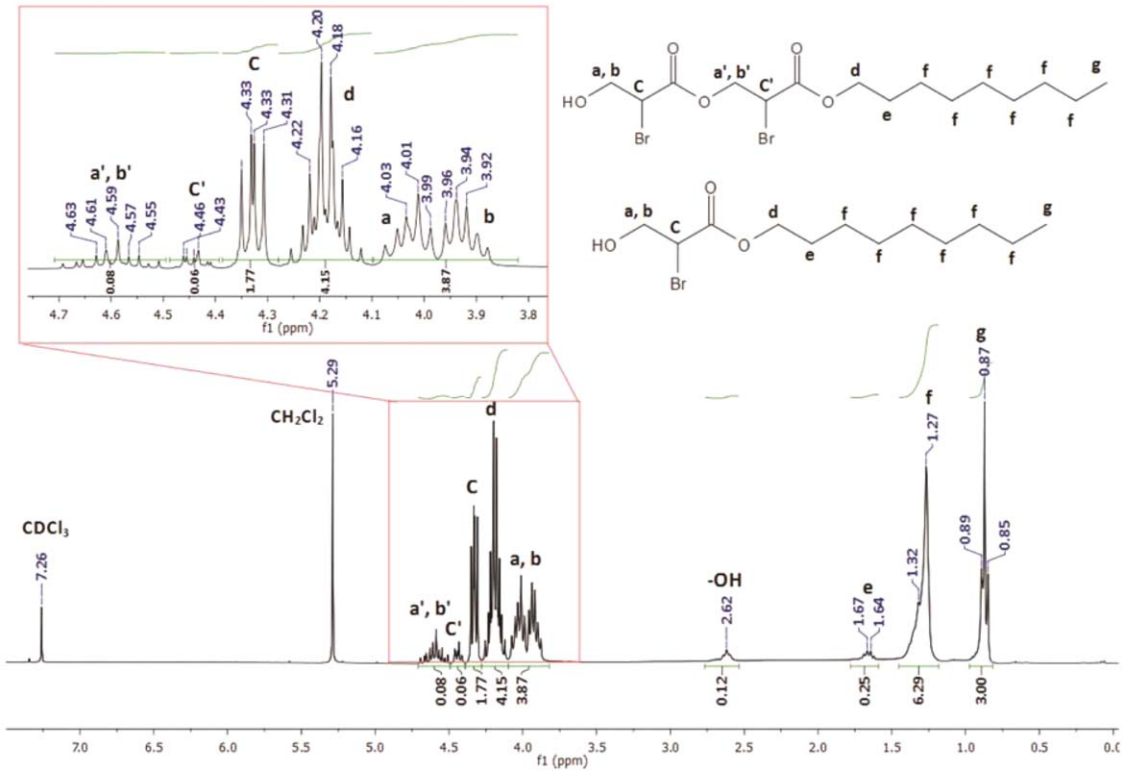

FIGURE 1 ^{1}H NMR (300 MHz) spectrum of *n*-nonyl 2-bromo-3-hydroxypropionate and its impurity formed by condensation oligomerization. [Color figure can be viewed in the online issue, which is available at wileyonlinelibrary.com.]

organic layers were washed four times with 4 wt % aqueous $NaHCO_3$ (50 mL each) and once with saturated aqueous NaCl (50 mL), and then dried over Na_2SO_4. After filtration and solvent removal by rotary evaporation, 16 g (63%) of crude product was obtained as a yellow liquid, and the crude product was purified by column chromatography ($R_f = 0.38$) using silica gel as the stationary phase and $CHCl_3$/hexanes (95:5 v/v) as the eluant to yield 13 g (52%) of (2-bromo-2-*n*-nonan-1-oxycarbonyl)ethyl acrylate as a colorless liquid.

^{1}H NMR: 0.87 (t, CH_3, $^3J = 6.6$ Hz,), 1.27 (m, [CH_2]$_6$), 1.66 (quint, CH_2CH$_2$O$_2$C, $J = 6.8$ Hz), 4.19 (m, CH_2O$_2$C), 4.43 (dd, CHBr, $^3J = 5.9$ Hz, $^3J = 8.1$ Hz), 4.53 (dd, CHHO$_2$C, $^2J = 11.4$ Hz, $^3J = 5.9$ Hz), 4.58 (dd, CHHO$_2$C, $^2J = 11.4$ Hz, $^3J = 8.1$ Hz), 5.88 (dd, CHH_b= trans to CO$_2$, $^2J_{ab} = 1.3$ Hz, $^3J_{bc} = 10.4$ Hz), 6.11 (dd, = CH_c, $^3J_{ac} = 17.3$ Hz, $^3J_{bc} = 10.4$ Hz), 6.44 (CH_aH= cis to CO$_2$, $^2J_{ab} = 1.3$ Hz, $^3J_{ac} = 17.3$ Hz). ^{13}C NMR: 14.4 (*C*H$_3$), 22.6 (*C*H$_2$CH$_3$), 25.7 (*C*H$_2$[CH$_2$]$_2$O$_2$C), 28.3 (*C*H$_2$CH$_2$O$_2$C), 29.1 (*C*H$_2$[CH$_2$]$_4$H), 29.2 (*C*H$_2$), 29.4 (*C*H$_2$[CH$_2$]$_3$H), 31.8 (*C*H$_2$CH$_2$CH$_3$), 40.7 (*C*HBr), 64.2 (*C*H$_2$CHBr), 66.5 (CO$_2$*C*H$_2$CH$_2$), 127.4 (*C*H=), 131.9 (*C*H$_2$=), 165.0 (acrylate *C*=O), 167.6 (*C*O$_2$CH$_2$).

Synthesis of n-Nonyl Acrylate

A solution of acryloyl chloride (3.8 g, 41 mmol) in dry CH_2Cl_2 (50 mL) was added dropwise over 30 min to a solution of *n*-nonanol (5.6 g, 39 mmol) and triethylamine (4.0 g, 40 mmol) in dry CH_2Cl_2 (100 mL). The reaction mixture was stirred at room temperature for 48 h, and then, the solvent was removed by rotary evaporation. The white residue was purified by column chromatography ($R_f = 0.57$) using silica gel as the stationary phase and CH_2Cl_2 as the eluant to yield 5.7 g (67%) of *n*-nonyl acrylate as a colorless liquid.

^{1}H NMR: 0.86 (t, CH_3, $^3J = 6.7$ Hz), 1.28 (m, [CH_2]$_6$), 1.67 (quint, CH_2CH$_2$O$_2$C, $J = 6.8$ Hz), 4.13 (t, OCH_2CH$_2$, $^3J = 6.7$ Hz), 5.78 (dd, CHH_b= trans to CO$_2$, $^2J_{ab} = 1.6$ Hz, $^3J_{bc} = 10.4$ Hz), 6.10 (dd, = CH_c, $^3J_{ac} = 17.3$ Hz, $^3J_{bc} = 10.4$ Hz), 6.37 (CH_aH= cis to CO$_2$, $^2J_{ab} = 1.6$ Hz, $^3J_{ac} = 17.3$ Hz).

ATRP of (2-Bromo-2-methoxycarbonyl)ethyl Acrylate for Screening Purposes

In a typical procedure, (2-bromo-2-methoxycarbonyl)ethyl acrylate (0.33 g, 0.97 mmol) was added under a stream of nitrogen to a well-stirred mixture of CuBr (7.5 mg, 52 μmol) and PMDETA (11 mg, 62 μmol) in anisole (0.6 mL) in a dry Schlenk tube, and the tube was sealed with a glass stopper. After stirring at room temperature for 10 min, the inimer mixture was degassed by five freeze–pump/30-min thaw cycles, and the polymerization tube was backfilled with N_2. The polymerization mixture was stirred at 130 °C for 9 h and then quenched by immersing the Schlenk tube into liquid N_2. The contents of the polymerization tube were thawed, exposed to the atmosphere, diluted with THF (7 mL), and precipitated into water/methanol (3/7 v/v, 30 mL). The precipitate was collected and reprecipitated twice from THF (10 mL) into water/methanol (3/7 v/v, 30 mL) to yield 46 mg (14%) hyperbranched PMA as a

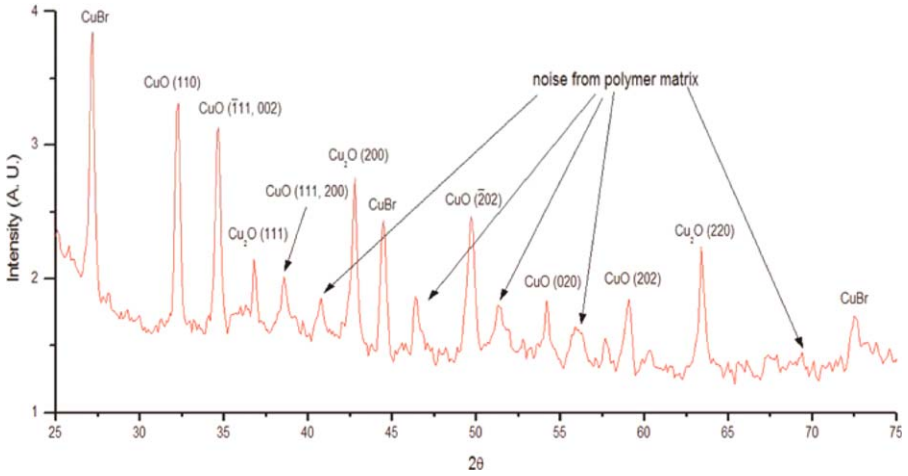

FIGURE 2 X-ray diffraction pattern of the brown-colored hyperbranched poly(*n*-nonyl acrylate) produced by atom transfer radical polymerization of (2-bromo-2-*n*-nonan-1-oxycarbonyl)ethyl acrylate system in anisole at 90 °C for 12 h using CuBr and PMDETA as the catalyst. [Color figure can be viewed in the online issue, which is available at wileyonlinelibrary.com.]

slightly yellow powder; $M_n = 1.00 \times 10^4$ g/mol, $Đ = 2.76$. The product was not purified further to remove copper catalyst(s).

ATRP of (2-Bromo-2-n-nonan-1-oxycarbonyl)ethyl Acrylate

A mixture of CuBr (6.2 mg, 42 μmol) and PMDETA (8.9 μL, 43 μmol) in anisole (0.5 mL) was sealed in a dry Schlenk tube with a rubber septum and degassed by five freeze–pump–thaw (5–15–10 min) cycles. Degassed (2-bromo-2-*n*-nonan-1-oxycarbonyl)ethyl acrylate (0.53 g, 1.5 mmol) was added to the catalyst mixture using a gas-tight syringe, and the polymerization tube was backfilled with N_2. The polymerization mixture was stirred at 90 °C for 12 h and then quenched by immersing the Schlenk tube into liquid N_2. The contents of the polymerization tube were thawed, exposed to the atmosphere, diluted with THF (5 mL), passed through a plug of basic activated alumina to remove the catalyst(s), and precipitated into methanol (25 mL). The precipitate was collected and reprecipitated twice from THF (5 mL) into methanol (25 mL) to yield 56 mg (48%) hyperbranched poly(*n*-nonyl acrylate) as a brown viscous rubber. As the brown color still remained after purification to remove copper catalyst(s), the polymer was not injected into the GPC for molecular weight analysis; X-ray diffraction (Fig. 2) confirmed that the sample contained trace amounts of CuBr, CuO (black),[31] and Cu_2O (red),[32] which evidently causes the brown color.

AGET ATRP of (2-Bromo-2-n-nonan-1-oxycarbonyl)ethyl Acrylate

In a typical procedure, (2-bromo-2-*n*-nonan-1-oxycarbonyl)-ethyl acrylate (0.53 g, 1.5 mmol) was added under a stream of nitrogen to a well-stirred mixture of $CuBr_2$ (6.6 mg, 30 μmol) and PMDETA (6 μL, 31 μmol) in acetonitrile (0.25 mL) in a dry Schlenk tube. The Schlenk tube was sealed with a glass stopper, and its contents were degassed by five freeze–pump–thaw (5–15–10 min) cycles. A saturated aqueous solution of ascorbic acid (16 μL, 30 μmol) was added using a gas-tight syringe, and the polymerization tube was backfilled with N_2. The polymerization mixture was stirred at 75 °C for 5 h and then quenched by immersing the Schlenk tube into liquid N_2. The contents of the polymerization tube were thawed, exposed to the atmosphere, diluted with THF, and passed through a plug of basic activated alumina to remove catalyst(s). The THF solution was concentrated to 5 mL and precipitated into methanol (25 mL). The precipitate was collected and reprecipitated three times from THF (5 mL) into methanol (25 mL) to yield 26 mg (48%) of hyperbranched poly(*n*-nonyl acrylate) as a white viscous gum; $M_n = 9.89 \times 10^3$ g/mol, $Đ = 8.91$.

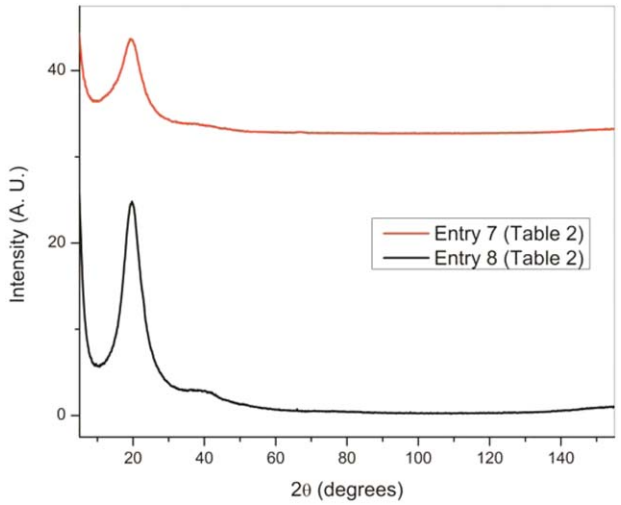

FIGURE 3 X-ray diffraction pattern of the hyperbranched poly(*n*-nonyl acrylate)s produced by activator generated by electron transfer (AGET) atom transfer radical polymerization of (2-bromo-2-*n*-nonan-1-oxycarbonyl)ethyl acrylate system at 60–75 °C using ascorbic acid as the reducing agent (Table 2, Entries 7 and 8). [Color figure can be viewed in the online issue, which is available at wileyonlinelibrary.com.]

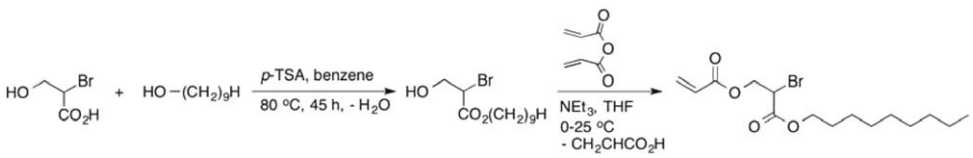

SCHEME 3 Synthesis of (2-bromo-2-*n*-nonan-1-oxycarbonyl)ethyl acrylate.

In contrast to the sample prepared by ATRP (Fig. 2), copper contaminants are not detectable by X-ray diffraction in the hyperbranched polymers isolated from these AGET ATRP (Fig. 3).

AGET ATRP Copolymerization of *n*-Nonyl Acrylate and (2-Bromo-2-*n*-nonan-1-oxycarbonyl)ethyl Acrylate

In a typical example, a solution of (2-bromo-2-*n*-nonan-1-oxycarbonyl)ethyl acrylate (0.27 g, 0.77 mmol) and *n*-nonyl acrylate (1.6 g, 8.0 mmol) was added to a well-stirred mixture of $CuBr_2$ (33 mg, 0.16 mmol) and PMDETA (33 μL, 0.16 mmol) in CH_3CN (1.25 mL) in a dry vial. The vial reactor was sealed with a rubber septum, and its contents were degassed by four freeze–pump–thaw (5–15–10 min) cycles. Solid ascorbic acid (27 mg, 0.16 mmol) was added to the frozen contents of the vial reactor. After one additional freeze–pump–thaw (5–15–10) cycle, the polymerization mixture was stirred at 75 °C for 8 days. The contents of the vial reactor were diluted with THF, decanted from the crosslinked gel in the bottom of the vial, and the solvent was removed *in vacuo* to yield 1.6 g (86%) yield of hyperbranched copolymer as a brownish viscous oil ($M_n = 5.11 \times 10^4$ g/mol, $Đ = 6.31$).

Crosslinking of Hyperbranched Poly(*n*-nonyl acrylate) In Situ

(2-Bromo-2-*n*-nonan-1-oxycarbonyl)ethyl acrylate (0.51 g, 1.5 mmol) was added under a stream of nitrogen to a well-stirred mixture of $CuBr_2$ (6.4 mg, 29 μmol) and PMDETA (6.6 μL, 31 μmol) in CH_3CN/H_2O (9/1 v/v, 0.5 mL) in a dry Schlenk tube. The Schlenk tube was sealed with a rubber septum, and its contents were degassed by five freeze–pump–thaw (5–15–10 min) cycles. A saturated aqueous solution of ascorbic acid (24 μL, 45 μmol) was added using a gas-tight syringe. The polymerization mixture was stirred at 75 °C for 1.8 h. As crosslinking occurred, the polymerization was quenched by immersing the Schlenk tube into liquid N_2. The contents of the polymerization tube were thawed, exposed to the atmosphere, and 0.52 g of crosslinked hyperbranched poly(*n*-nonyl acrylate) was isolated as a yellowish gummy material by filtration and drying *in vacuo* for 2 days. Copper catalysts and soluble materials were extracted three times from the gummy material by immersing it in a solution of triethylamine (three drops) in THF (10 mL) for 4 days each to obtain 0.28 g (>55% yield) of a yellowish crosslinked polymer; the yield is underestimated because the amount of bromine atoms lost is not known.

Crosslinking of Preformed Hyperbranched Poly(*n*-nonyl acrylate) (Two-Step Procedure)

A mixture of CuBr (6.5 mg, 31 μmol) and AIBN (19 mg, 0.12 mmol) in anisole (1 ml) was sealed in a dry Schlenk tube with a rubber septum and degassed by four freeze–pump–thaw cycles. A second Schlenk tube containing hyperbranched poly(*n*-nonyl acrylate) (0.53 g, $M_n = 1.56 \times 10^4$ g/mol, $Đ = 6.26$) in anisole (20 mL) was sealed with a rubber septum and degassed by four freeze–pump–thaw (5–15–10 min) cycles. After the addition of PMDETA (6.8 μL, 32 μmol) to the polymer solution via a gas-tight syringe, an aliquot of the polymer solution (5 mL, ~13 μmol/L) was transferred via a cannula to the catalyst solution. The Schlenk tube was then backfilled with N_2, and the contents were stirred at 75 °C for 92 h. The resulting green insoluble powder (43 mg, 32% yield) was collected in a glass frit.

RESULTS AND DISCUSSION

Synthesis of the (2-Bromo-2-*n*-nonan-1-oxycarbonyl)ethyl Acrylate Inimer

As outlined in Scheme 3, (2-bromo-2-*n*-nonan-1-oxycarbonyl)-ethyl acrylate was synthesized by esterification of 2-bromo-3-hydroxypropionic acid with *n*-nonyl alcohol, followed by esterification of the resulting *n*-nonyl 2-bromo-3-hydroxypropionate with acrylic anhydride, similar to our previous synthesis of (2-bromo-2-methoxycarbonyl)ethyl acrylate.[9] Figure 4 presents the ^{1}H NMR spectrum of the *n*-nonyl inimer. In addition to the resonances at 5.88 ppm (dd, CH*H*= trans to CO_2), 6.11 ppm (dd, =C*H*), and 6.44 ppm (C*H*H= cis to CO_2) due to the acrylate double bond, the most characteristic ^{1}H resonances of the inimer are those at 4.43 ppm due to the C*H*Br methine, and at 4.53 ppm and 4.58 ppm due to the diastereotopic methylene protons alpha to the brominated carbon. Figure 5 presents the corresponding ^{13}C NMR spectrum. In addition to the resonances at 127.4 ppm (*C*H=), 131.9 ppm (*C*H_2=), and 165.0 ppm (acrylate *C*=O), the most characteristic ^{13}C resonances of the inimer are those at 40.7 ppm (*C*HBr) and 66.5 ppm (*C*H_2O_2C).

Polymerizations

We previously demonstrated that the methyl acrylate inimer could be polymerized by both ATRP and reverse ATRP,[8] although the conditions were not optimized. We therefore briefly screened the ATRP of the methyl bromoinimer as a function of time and concentration to determine when the growing polymer starts to crosslink and gel under standard ATRP conditions. As demonstrated by Entries 1 and 2 in Table 1, the hyperbranched PMA remained soluble at short polymerization times (≤9 h), but underwent radical–radical crosslinking when the polymerization time increased to 14 h. In solution using anisole as the solvent, crosslinking evidently involved significant intermolecular crosslinking, as

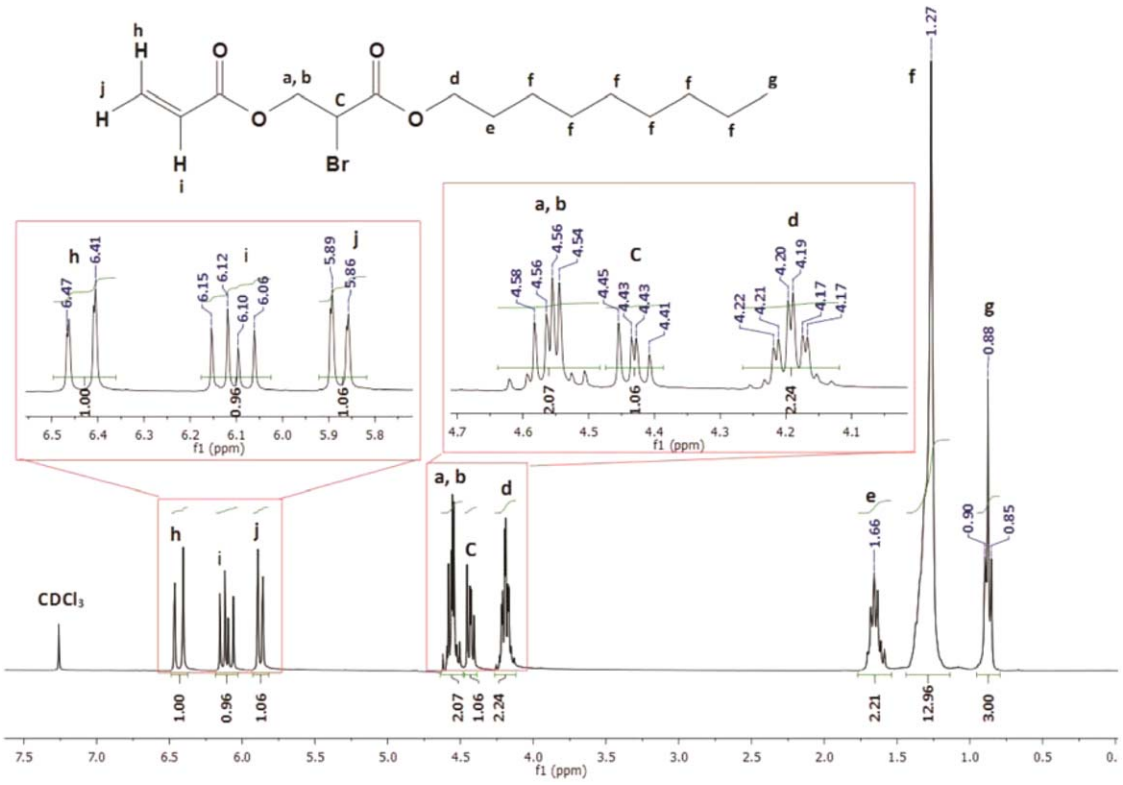

FIGURE 4 ^{1}H NMR (300 MHz) spectrum of (2-bromo-2-*n*-nonan-1-oxycarbonyl)ethyl acrylate. [Color figure can be viewed in the online issue, which is available at wileyonlinelibrary.com.]

well as intramolecular crosslinking, as the polymerization resulted in the formation of an insoluble gel. Surprisingly, in the absence of solvent, the polymerization resulted in small, hard plastic particles at long reaction times, evidently due to extensive intramolecular crosslinking. The lack of macrogel formation under more concentrated (bulk) conditions may be explained by the high rate of radical–radical coupling, which rapidly resulted in insoluble particles that were not able to further react with other partially crosslinked molecules in the system.

The bulky *n*-nonyl substituent should decrease the rates of reactions of the new *n*-nonyl acrylate inimer relative to those of the methyl inimer. As summarized in Table 2, we therefore briefly screened ATRP and AGET ATRP conditions to determine under what conditions the growing hyperbranched poly(*n*-nonyl acrylate) starts to crosslink and gel. The brownish color of the sample in Entry 1 indicates that copper salts remain in the polymer produced in anisole at 90 °C within 12 h under standard ATRP conditions; X-ray diffraction confirmed that this sample contained trace amounts of CuBr,

FIGURE 5 ^{13}C NMR (75 MHz) spectrum of (2-bromo-2-*n*-nonan-1-oxycarbonyl)ethyl acrylate.

TABLE 1 Cursory Results from the Atom Transfer Radical Polymerization of (2-Bromo-2-methoxycarbonyl)ethyl Acrylate at 130 °C[a]

Entry	Solvent	Reaction Time	Observation
1	Anisole	9 h	Hyperbranched polymer[b]
2	Anisole	14 h	Swollen gel
3	–	4 days	Hard particles

[a] [Inimer]:[CuBr]:[PMDETA] = 17–19:1:1.
[b] $M_n = 1.00 \times 10^4$ g/mol, $Đ = 2.76$.

CuO, and Cu_2O (Fig. 2). The very low yields of insoluble powders in Entries 2–4 demonstrate that DMF is not a good solvent for this polymerization under both standard ATRP and AGET ATRP conditions at 60–75 °C, as highly crosslinked powders formed before the polymerization reached high conversion, evidently due to the generation of a high concentration of radicals in this very polar solvent. Entries 5 and 6 demonstrate that the rate of reduction of Cu(II) with Cu(0) was too slow for an effective AGET ATRP, as no polymer was obtained. However, Entries 7 and 8 demonstrate that ascorbic acid is a promising reducing agent for AGET ATRP of the *n*-nonyl inimer in acetonitrile and a mixture of acetonitrile and water, as crosslinking does not occur until high conversions. In these two cases, no copper was detected in the isolated samples by X-ray diffraction (Fig. 3).

The results of the AGET ATRP of 50 equivalents of (2-bromo-2-*n*-nonan-1-oxycarbonyl)ethyl acrylate relative to $CuBr_2$ in solutions of 9:1 (v/v) acetonitrile and water at 75 °C are summarized in Table 3. The broad polydispersities are characteristic of hyperbranched polymers produced by SCVPs due to propagation by both step and chain mechanisms.[13,14] Comparison of Entries 1–3 demonstrates that the highest yield of soluble hyperbranched polymer was produced using a ratio of 1:1 [$CuBr_2$]:[ascorbic acid]. Higher concentrations of ascorbic acid (Entry 4) and inimer (Entries 5 and 6) resulted in faster polymerization rates that led to uncontrolled crosslinking by radical–radical coupling, and therefore little soluble polymer. When water was eliminated from the solvent system (Entry 7), the polymerization rate decreased, and a relatively high yield of soluble polymer was obtained at a short reaction time. (2-Bromo-2-*n*-nonan-1-oxycarbonyl)-ethyl acrylate also copolymerized well with *n*-nonyl acrylate using the same conditions. For example, a copolymerization of 1:10 inimer/monomer produced an 86% yield of hyperbranched copolymer that was still soluble after 8 days at 75 °C in acetonitrile using 1:1:1 [$CuBr_2$]/[PMDETA]/[AA] and 55 equivalents of acrylate groups.

Figure 6 presents the ^{1}H NMR spectrum of the hyperbranched poly(*n*-nonyl acrylate) reported as Entry 1 in Table 3. As is typical of these hyperbranched polyacrylates,[9,10] the terminal vinyl resonances appear at 5.75–6.5 ppm; the CO_2CH_2CHBr and $CHBr$ resonances of the acrylate ester portion of the polymer overlap at 4.5 ppm; and the CH_2O_2C resonance of the *n*-nonyl ester pendant groups appear at 3.9 ppm. The backbone protons resonate in the region from 1 to 3.5 ppm, under the prominent resonances at 0.8 ppm (CH_3), 1.25 (—$[CH_2]_6$—) ppm, and 1.7 ppm ($CH_2CH_2O_2C$) due to the *n*-nonyl ester pendant groups. All of the resonances are broad, as expected for a polymer, and no unique resonances are detected for the branch points; therefore, the degree of branching cannot be calculated for these hyperbranched polyacrylates by NMR spectroscopy.[10]

One-Pot *In Situ* versus Two-Step Crosslinking

As summarized in Table 4, we compared two approaches for crosslinking the hyperbranched poly(*n*-nonyl acrylate)s by ATRC of the activated carbon–bromine bonds that are present throughout the hyperbranched structure. In the first route, the hyperbranched polymer was crosslinked in one pot, *in situ* during its synthesis due to the inevitable radical–radical coupling at high inimer conversion. The second route used a two-step process in which the carbon–bromine bonds of a preformed hyperbranched polymer were activated under ATRC conditions, and the resulting radicals were coupled.

TABLE 2 Cursory Results from the ATRP and AGET ATRP of (2-Bromo-2-*n*-nonan-1-oxycarbonyl)ethyl Acrylate under Various Conditions[a]

Entry	[In]:[CuBr]:[$CuBr_2$][b]	Reducing Agent	[Reducing Agent]/[$CuBr_2$]	Solvent	Temperature (°C)	Time (h)	% Yield (Observations)
1	35/1/0	–	–	Anisole	90	12	45 (brown soluble polymer)
2	47/1/0	–	–	DMF	60	40	(Insoluble hard particles)
3	52/0/1.6	AA	1.6	DMF	70	13	2 (hard particles)
4	50/0/1	AA	1	DMF	75	18	2 (hard particles)
5	43/0/0.9	Cu(0)	1.3	9:1 CH_3CN/H_2O	75	24	0
6	50/0/1	Cu(0)	1.5	DMSO	25	74	0
7	40/0/1	AA	2.3	5:1 CH_3CN/H_2O	60	15	13 (pseudo-crosslinked)[c]
8	50/0/1	AA	2	CH_3CN	75	27	Crosslinked gel

[a] Inimer concentration = [In] = 3 mmol/mL; AA, ascorbic acid.
[b] Relative to 1 equiv *N,N,N′,N″,N″*-pentamethyldiethylenetriamine (PMEDTA).
[c] Pseudo-crosslinked refers to a poorly soluble, swollen gel that dissolved almost completely after extensive time in a good solvent; in this case, $M_n = 7.04 \times 10^4$, $Đ = 4.62$.

TABLE 3 Results from AGET ATRP of (2-Bromo-2-*n*-nonan-1-oxycarbonyl)ethyl Acrylate under Various Conditions in 9:1 (v/v) CH_3CN/H_2O at 75 °C[a]

Entry	[$CuBr_2$]/[PMDETA]/[AA]	[Inimer] (mmol/mL)	Time (h)	% Yield[b]	$M_n \times 10^{-4}$	$Đ$
1	1:1:1	3	20	25	1.56	6.26
2	1:1:0.5	3	120	2	0.445	1.46
3	1:1:0.8	3	23	16	5.09	2.86
4	1:1:1.3	3	18	[c]	2.56	2.70
5	1:1:1	8	0.5	[c]	12.1	3.41
6	1:1:1	6	1	[c]	10.4	3.11
7[d]	1:1:1	6	5	48	9.89	8.91

[a] [Inimer]/[$CuBr_2$] = 50; AA, ascorbic acid.
[b] After precipitation and three reprecipitations to remove any unreacted inimer.
[c] Small amount of soluble polymer extracted from crosslinked material.
[d] In acetonitrile without water.

Surprisingly, the two-step reaction produced insoluble, highly crosslinked powders rather than a lighter crosslinked swollen gel from both a homopolymer of the inimer (Entry 1b) and a copolymer (Entry 2b) in which the number of crosslinkable sites were diluted using 10 equivalents of *n*-nonyl acrylate. As exemplified in Figure 7(b), the resulting powders were not soluble in THF or water (which were used to extract copper catalysts and/or ligand); the greenish color in THF and bluish color in water is due to the extraction of copper ions. The lack of macrogel formation again indicates that the rate of radical–radical coupling was too high, and the crosslinked particles rapidly precipitated out of the solution before they were able to react intermolecularly with other partially crosslinked molecules in the system.

Crosslinking is evidently slower in the one-pot method using AGET ATRP conditions. In this case, a gel formed from the entire reaction mixture using both a homopolymerization (Entry 1a), which therefore results in a high concentration of crosslinkable sites, and a copolymerization of inimer diluted with 10 equivalents of *n*-nonyl acrylate (Entry 2a). As demonstrated by the example in Figure 7(a), the resulting crosslinked poly(*n*-nonyl acrylate)s act as organogels and swell in THF. The swelling ratio of the gel, as determined by the weight of the swollen gel divided by the weight of the dried gel, increased as the crosslink density decreased as a result of copolymerization with the acrylate monomer. No crosslinking occurred when the density of crosslinkable sites was further decreased by copolymerization of the inimer with 50 equivalents of acrylate monomer.

*Characterization of Crosslinked Poly(*n*-nonyl acrylate)*

The thermal behavior of a representative dry gel (Table 2, Entry 8) resulting from a hyperbranched homopolymer of poly(*n*-nonyl acrylate) was characterized by differential scanning calorimetry (Fig. 8) and thermal gravimetric analysis (Fig. 9). As shown in Figure 8, the dry gel exhibits a low-temperature glass transition at −50 °C, evidently due to the long *n*-nonyl ester substituents, which decrease chain packing. The T_g of the dry gel is similar to that of linear poly(*n*-nonyl acrylate) ($T_g = -57$ °C).[33] However, the steady change in the baseline at lower temperature indicates that the glass

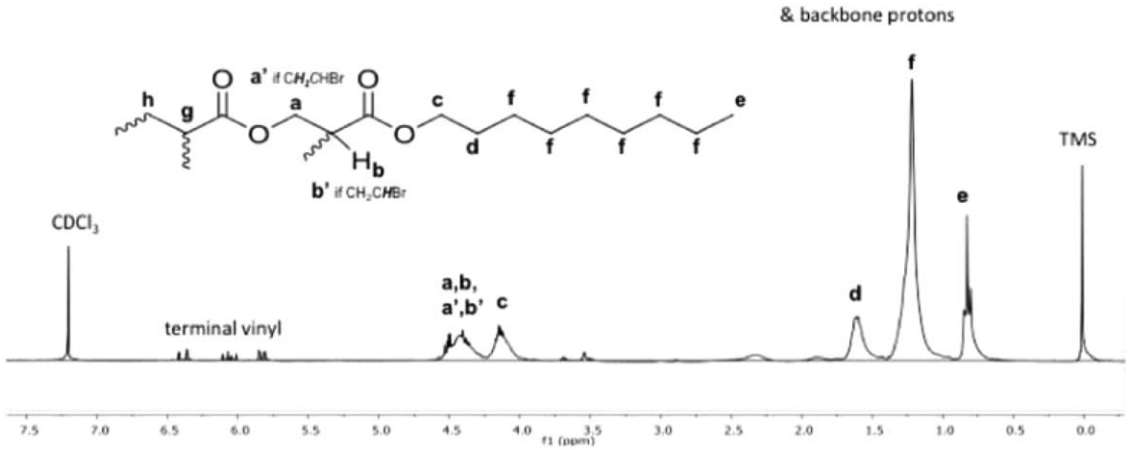

FIGURE 6 ^{1}H NMR (300 MHz) spectrum of hyperbranched poly(*n*-nonyl acrylate) produced by AGET atom transfer radical polymerization of (2-bromo-2-*n*-nonan-1-oxycarbonyl)ethyl acrylate in 9:1 (v/v) CH_3CN/H_2O at 75 °C (Table 3, Entry 1).

TABLE 4 Results of One-Pot versus Two-Step Crosslinking of Hyperbranched Poly(*n*-nonyl acrylate) with Varying Concentrations of Crosslinkable Sites

Entries	[Inimer]/[M][a]	One-Step Crosslinking		Two-Step Crosslinking
		Product	Swelling Ratio[b]	
1a and 1b	1/0	Gel	4	Plastic particles
2a and 2b	1/10	Gel	34	Plastic particles
3a	1/50	No crosslinking		–

[a] M = monomer (*n*-nonyl acrylate).

[b] Swelling ratio = weight of swollen gel/weight of dry crosslinked polymer.

transition may cover a broader range of temperatures, possibly due to both the nonuniform structure of hyperbranched polymers and the inherent irregularity of crosslinking. As shown by the TGA scan in Figure 9, the dry gel is quite thermally stable in air up to 150 °C; therefore, its viscoelastic behavior can be studied at temperatures up to at least 100 °C without degradation occurring. The dry gel starts to slowly degrade at temperatures above 150 °C, with 3 wt % loss at 275 °C. Degradation is rapid at temperatures above 325 °C.

The viscoelastic behavior of the same dry gel at 1% strain is shown by the dynamic shear data in Figure 10. The elastic modulus (G') exhibited a relatively weak frequency dependence, whereas the loss modulus (G'') showed a stronger frequency dependence in the frequency range of 0.001–100 rad/s. Moreover, $G' > G''$ for all frequencies studied at 25 °C. This indicates that the material is a viscoelastic solid at 25 °C, and the data in Figure 10 are consistent with a time-dependent network. The magnitude of G' (10^3 to 10^4 Pa) is consistent with that of a soft gel. The frequency dependence of G' in Figure 10 is indicative of a weak network that would arise as a result of physical, reversible crosslinks; defects in a covalently crosslinked network,[34] such as dangling chains formed during the crosslinking step or random crosslinking of reactive ends of propagating hyperbranched polymer; or a combination of chemical and physical crosslinks with or without defects. The G'' frequency dependence in Figure 10 is expected to have a slope of 1 for a material exhibiting viscous flow; the higher slope of the G'' frequency dependence demonstrates that the dry gel is a rubbery-like solid and not a liquid.

The data in Figure 10 cannot distinguish between a network containing covalent crosslinks and a physical network simply of chain entanglements or weak physical crosslinks. The stress relaxation data in Figure 11 resolve this uncertainty. If the network structure for the sample characterized in Figure 10 was only due to physical crosslinks or chain entanglements, the stress in a relaxation experiment should go to zero as time goes to infinity. The stress relaxation results shown in Figure 11 were run for nearly 14 h, and the stress is clearly approaching a finite value, G_{inf}, as expected for a covalently crosslinked polymer.[34] Moreover, the theory of rubber elasticity predicts that the modulus, in this case, G_{inf}, should scale linearly with temperature.[35]

G_{inf} was determined for the data in Figure 11 by fitting a stretched exponential[36] to the data,

$$G(t) = a + b[exp(-t/c)^d], \quad (1)$$

where a is the equilibrium relaxation modulus (G_{inf}), which is zero for a liquid and finite for a solid, c is a characteristic

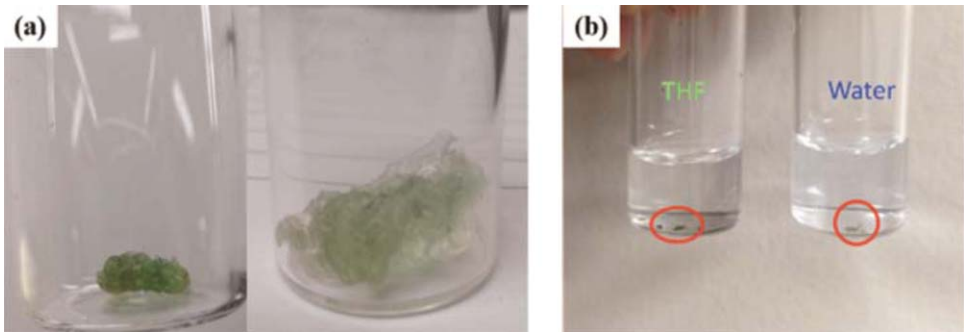

FIGURE 7 (a) Crosslinked gel of hyperbranched poly(*n*-nonyl acrylate) formed *in situ* during the copolymerization of 1:10 inimer:monomer before (left) and after swelling (right; swelling ratio = 34) in THF. (b) Insoluble crosslinked hard particles (red circles) of hyperbranched poly(*n*-nonyl acrylate) (Table 4, Entry 1b) formed by crosslinking preformed homopolymer after 6 h swelling time in THF (5 mL) and in water (5 mL). [Color figure can be viewed in the online issue, which is available at wileyonlinelibrary.com.]

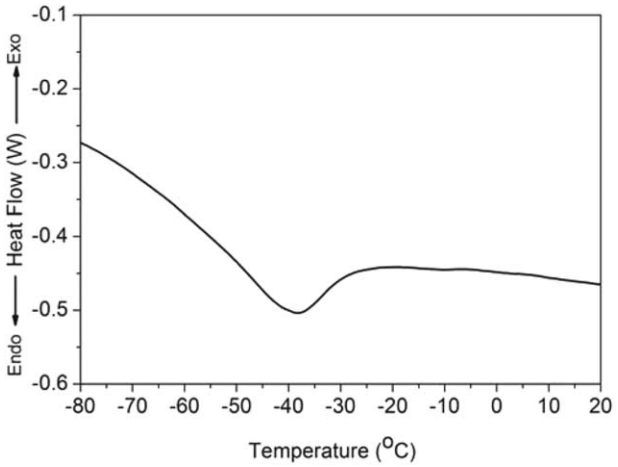

FIGURE 8 Differential scanning calorimetry trace (10 °C/min; third heating scan, which is equivalent to the first and second heating scans) of dry gel (Table 2, Entry 8).

relaxation time, d is a stretching parameter, which is a function of the distribution of relaxation times ($0 < d < 1$), and $b = G(\text{inf}) - G(0)$. This equation is often used to represent relaxation data where there is a wide distribution of relaxation times. The stretched exponential provides a simple fit to data with many relaxation times, although it sacrifices the ability to determine specific relaxation times; that is, instead a single relaxation time is determined. The solid lines in Figure 11 are the model fits, and the parameters for the four sets of data are summarized in Table 5.

The values of $a = G_{\text{inf}}$ increased with temperature, and the characteristic relaxation time, c, was independent of temperature until the temperature reached 100 °C. The theory of rubber elasticity predicts that the modulus, in this case, G_{inf}, should scale linearly with temperature.[37] The inset in Figure 11 shows that the temperature dependence of G_{inf} is linear, which is consistent with rubber elasticity theory. This result confirms that these samples are covalently crosslinked.

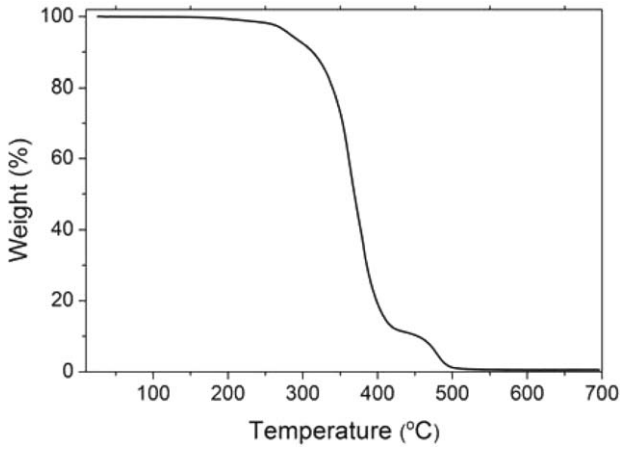

FIGURE 9 Thermal gravimetric analysis scan (10 °C/min) of dry gel (Table 2, Entry 8) in air.

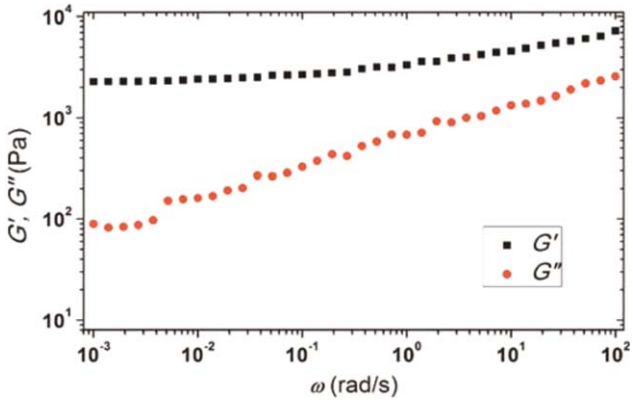

FIGURE 10 Variation of storage modulus (G') and loss modulus (G'') of dry gel (Table 2, Entry 8) as a function of angular frequency (ω) at 25 °C. [Color figure can be viewed in the online issue, which is available at wileyonlinelibrary.com.]

CONCLUSIONS

The acrylate inimer, (2-bromo-2-*n*-nonan-1-oxycarbonyl)ethyl acrylate, can be polymerized and copolymerized with *n*-nonyl acrylate to high molecular weight in a relatively short time by AGET ATRP (co)polymerization in acetonitrile at 75 °C using 1:1:1 $CuBr_2$]/[PMDETA]/[ascorbic acid]. The resulting hyperbranched poly(*n*-nonyl acrylate)s are readily crosslinked via the many bromine atoms throughout the structure. However, crosslinking of preformed hyperbranched polymers generate hard plastic powders under ATRC conditions, evidently due to rapid radical–radical coupling, which does not allow partially crosslinked material to remain in solution long enough to undergo sufficient intermolecular

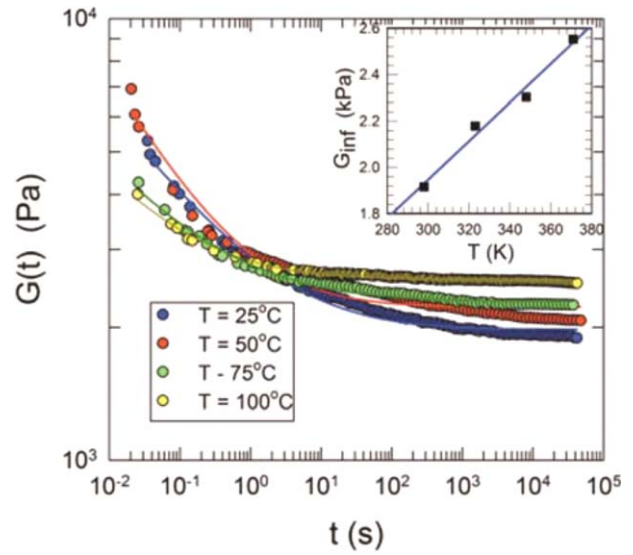

FIGURE 11 Stress relaxation behavior of dry gel (Table 2, Entry 8) at four different temperatures. The inset shows the temperature dependence of G_{inf}. The data curves correspond from top to bottom at long time (10^4 s): 100 °C (top) and 75 °C, 50 °C, and 25 °C (bottom). [Color figure can be viewed in the online issue, which is available at wileyonlinelibrary.com.]

TABLE 5 Fitting Parameters for Using eq 1 $\{G(t)=a+b\ [\exp(-t/c)^d]\}$ Used to Fit the Data in Figure 11

	25 °C	50 °C	75 °	100 °C
a (Pa)	1,917	2,179	2,302	2,552
b (Pa)	943	767	420	275
d	0.950	0.950	0.950	0.872
c (s)	1.163	0.9538	0.8896	0.8541

crosslinking. To form a gel rather than small plastic particles, the rate of crosslinking must be decreased, which is more readily achieved in one pot in solution at high inimer conversions during the synthesis of hyperbranched polymers and copolymers. The resulting crosslinked polymers are hydrophobic due to the *n*-nonyl ester substituents and act as organogels that swell in THF. The swelling ratio increases as the number of crosslinks in the gel decreases, which was achieved by copolymerization with a standard acrylate monomer (*n*-nonyl acrylate). Without solvent, the dry network behaves as a viscoelastic solid with a glass transition at −50 °C. The linear temperature dependence of G_{inf} confirms that the dry networks are covalently crosslinked.

ACKNOWLEDGMENTS

This work was supported by the National Science Foundation through CHE-1112326 and CMMI-1300212. The authors thank Jing Wang and Professor Stephen Z. D. Cheng for the X-ray scattering analyses.

REFERENCES AND NOTES

1 J. S. Wang, K. Matyjaszewski, *Macromolecules* **1995**, *28*, 7572–7573.

2 T. E. Patten, J. Xia, T. Abernathy, K. Matyjaszewski, *Science* **1996**, *272*, 866–868.

3 M. J. Ziegler, K. Matyjaszewski, *Macromolecules* **2001**, *34*, 415–424.

4 J. M. J. Frechet, M. Henmi, I. Gitsov, S. Aoshima, M. R. Leduc, R. B. Grubbs, *Science* **1995**, *269*, 1080–1083.

5 K. Matyjaszewski, S. G. Gaynor, A. Kulfan, M. Podwika, *Macromolecules* **1997**, *30*, 5192–5194.

6 K. Matyjaszewski, S. G. Gaynor, *Macromolecules* **1997**, *30*, 7042–7049; (b) K. Matyjaszewski, J. Pyun, S. G. Gaynor, *Macromol. Rapid Commun.* **1998**, *19*, 665–670.

7 C. Gao, D. Yan, *Prog. Polym. Sci.* **2004**, *29*, 183–275.

8 C. Pugh, A. Singh, *WO2008045299-A1*, **2008**; (b) C. Pugh, A. Singh, *U.S. Patent 8,524,942*, **2013**.

9 C. Pugh, B. Raveendra, A. Singh, R. Samuel, G. Garcia, *Synlett.* **2010**, *13*, 1947–1950.

10 C. Pugh, A. Singh, R. Samuel, K. M. Bernal Ramos, *Macromolecules* **2010**, *43*, 5222–5232.

11 K. Chaicharoen, M. J. Polce, A. Singh, C. Pugh, C. Wesdemiotis, *Anal. Bioanal. Chem.* **2008**, *392*, 595–607.

12 W. Jakubowski, K. Matyjaszewski, *Macromolecules* **2005**, *38*, 4139–4146.

13 A. H. E. Müller, D. Yan, M. Wulkow, *Macromolecules* **1997**, *30*, 7015–7023.

14 D. Yan, A. H. E. Müller, K. Matyjaszewski, *Macromolecules* **1997**, *30*, 7024–7033.

15 T. M. Don, M. L. Huang, A. C. Chiu, K. H. Kuo, W. Y. Chi, *Mater. Chem. Phys.* **2008**, *107*, 266–273.

16 P. R. Ninawe, S. J. Parulekar, *Ind. Eng. Chem. Res.* **2012**, *51*, 1741–1755.

17 C. M. Sahagun, S. E. Morgan, *ACS Appl. Mater. Interfaces* **2012**, *4*, 564–572.

18 P. Terech, R. G. Weiss, *Chem. Rev.* **1997**, *97*, 3133–3159.

19 D. Dasgupta, J. M. Guenet, *Macromol. Chem. Phys.* **2012**, *214*, 1885–1892.

20 Y. Wu, T. Zhang, Z. Xu, Q. Guo, *J. Mater. Chem. A* **2015**, *3*, 1906–1909.

21 R. Kumar, O. P. Katare, *AAPS Pharm. Sci. Tech.* **2005**, *6*, E298–E310.

22 P. Rajamalli, E. Prasad, *Org. Lett.* **2011**, *13*, 3714–3717.

23 X. Cao, T. Zhang, A. Gao, K. Li, Q. Cheng, L. Song, M. Zhang, *Org. Biomol. Chem.* **2014**, *12*, 6399–6405.

24 Y. Liu, A. Lloyd, G. Guzman, K. A. Cavicchi, *Macromolecules* **2011**, *44*, 8622–8630.

25 S. Yurteri, I. Cianga, Y. Yagci, *Macromol. Chem. Phys.* **2003**, *204*, 1771–1783.

26 T. Sarbu, K. Y. Lin, J. Ell, D. J. Siegwart, J. Spanswick, K. Matyjaszewski, *Macromolecules* **2004**, *37*, 3120–3127.

27 T. Sarbu, K. Y. Lin, J. Spanswick, R. R. Gil, D. J. Siegwart, K. Matyjaszewski, *Macromolecules* **2004**, *37*, 9694–9700.

28 C. F. Huang, Y. Ohta, A. Yokoyama, T. Yokozawa, *Macromolecules* **2011**, *44*, 4140–4148.

29 M. N. C. Balili, T. Pintauer, *Inorg. Chem.* **2010**, *49*, 5642–5649.

30 R. N. Keller, H. D. Wycoff, *Inorg. Synth.* **1946**, *2*, 1–4.

31 J. F. Xu, W. Ji, Z. X. Shen, S. H. Tang, X. R. Ye, D. Z. Jia, X. Q. Xin, *J. Solid State Chem.* **1999**, *147*, 516–519.

32 M. Salavati-Niasari, F. Davar, *Mater. Lett.* **2009**, *63*, 441–443.

33 A. R. Katritzky, S. Sild, V. Lobanov, M. Karelson, *J. Chem. Inf. Comput. Sci.* **1998**, *38*, 300–304.

34 M. Rubinstein, R. Colby, Polymer Physics, 1st ed.; Oxford University Press; New York, **2003**; Chapter *7*, p 293.

35 A. V. Tobolsky, D. W. Carlson, N. Indictor, *J. Polym. Sci.* **1961**, *54*, 175–192.

36 G. Williams, D. C. Watts, *Trans. Faraday Soc.*, **1970**, *66*, 80–85.

37 M. Rubinstein, R. Colby, *Polymer Physics*, 1st ed.; Oxford University Press; New York, **2003**; Chapter *9*, p 362.